ACS Energy LETTERS

http://pubs.acs.org/journal/aelccp

LETTER

Electrolysis of CO_2 to Syngas in Bipolar Membrane-Based Electrochemical Cells

Yuguang C. Li,[†] Dekai Zhou,[†] Zhifei Yan,[†] Ricardo H. Gonçalves,[†] Danielle A. Salvatore,[‡] Curtis P. Berlinguette,[‡] and Thomas E. Mallouk*[,†]

[†]Departments of Chemistry, Biochemistry and Molecular Biology, and Physics, The Pennsylvania State University, University Park, Pennsylvania 16802, United States

[‡]Departments of Chemistry and Chemical and Biological Engineering, University of British Columbia, Vancouver, BC V6T 1Z2, Canada

Supporting Information

ABSTRACT: The electrolysis of CO_2 to syngas ($CO + H_2$) using nonprecious metal electrocatalysts was studied in bipolar membrane-based electrochemical cells. Electrolysis was carried out using aqueous bicarbonate and humidified gaseous CO_2 on the cathode side of the cell, with Ag or Bi/ionic liquid cathode electrocatalysts. In both cases, stable currents were observed over a period of hours with an aqueous alkaline electrolyte and $NiFeO_x$ electrocatalyst on the anode side of the cell. In contrast, the performance of the cells degraded rapidly when conventional anion- and cation-exchange membranes were used in place of the bipolar membrane. In agreement with earlier reports, the Faradaic efficiency for CO_2 reduction to CO was high at low overpotential. In the liquid-phase bipolar membrane cell, the Faradaic efficiency was stable at about 50% at 30 mA/cm^2 current density. In the gas-phase cell, current densities up to 200 mA/cm^2 could be obtained, albeit at lower Faradaic efficiency for CO production. At low overpotentials in the gas-phase cathode cell, the Faradaic efficiency for CO production was initially high but dropped within 1 h, most likely because of dewetting of the ionic liquid from the Bi catalyst surface. The effective management of protons in bipolar membrane cells enables stable operation and the possibility of practical CO_2 electrolysis at high current densities.

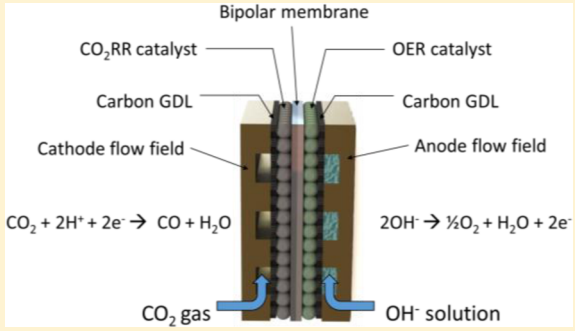

The reduction of carbon dioxide to fuels and chemicals is a problem of great importance for a sustainable energy future. Much of the current research on this problem is being directed toward the development of heterogeneous and homogeneous catalysts that selectively produce carbon monoxide, formate, methanol, and carbon-coupled products from CO_2.[1−11] While these studies have contributed to our understanding of the electrolytic cathode reactions, relatively little research has been devoted to system-level issues that are essential to the efficient and continuous operation of CO_2 electrolyzers.

In CO_2 electrolyzers, the CO_2 reduction reaction (CO_2RR) is paired with the oxygen evolution reaction (OER). The OER occurs most efficiently under strongly alkaline conditions with non-noble metal catalysts.[12,13] In contrast, the CO_2RR occurs most efficiently under acidic, nonaqueous conditions (e.g., in the presence of alkylimidazolium ions that stabilize the CO_2^- intermediate)[10,14−17] or in aqueous bicarbonate solutions.[6,7] These reactions have been studied in electrolyzers with cation- or anion-exchange membranes in order to prevent the mixing of anolyte and catholyte solutions.[6,18−22] In these systems, the simultaneous requirements for selective ion transport through the membrane (to maintain constant solution pH on both sides[23]) and the inhibition of product crossover create significant constraints. For example, if a cation exchange membrane is used, the anode must operate in acid, requiring expensive OER catalysts based on precious metals. With anion exchange membranes, bicarbonate electrolytes are typically used, resulting in less efficient anode performance and increasing the rate of products crossover, especially of neutral and anionic products such as methanol and formate, from the cathode to the anode. Some composite membrane structures have been studied to address these problems. Most notably, Delacourt et al. studied systems for the gas-phase CO_2RR in which a bicarbonate buffer layer separated the cathode from the cation-exchange membrane.[18] While this arrangement enabled the stable operation of the cell, it required a Pt−Ir anode catalyst, and it also entailed a free-energy loss associated with the acid−base neutralization reaction of H^+ and HCO_3^- at the interface between the cation exchange membrane and the buffer layer.

Received: September 26, 2016
Accepted: November 8, 2016
Published: November 8, 2016

DOI: 10.1021/acsenergylett.6b00475
ACS Energy Lett. 2016, 1, 1149−1153

Bipolar membranes (BPM) consist of anion- and cation-exchange membranes that are laminated together, typically with a catalyst that promotes the autodissociation of water at the interface. Under reverse bias conditions, BPM-based electrolysis cells can maintain constant pH on the two sides by the selective transport of H^+ and OH^- ions to the cathode and anode, respectively.[24−30] BPM-based electrolyzers coupled to photovoltaic cells have been designed to split water with high efficiency.[24] Very recently, Zhou et al. demonstrated the efficient conversion of bicarbonate to formate in a BPM-based photoelectrochemical cell that contained a nonprecious metal photoanode operated under alkaline conditions.[31]

In this study, we designed a CO_2 electrolyzer system based on a commercial BPM with an alkaline $NiFeO_x$ OER catalyst. We studied CO_2 electrolysis with both Ag/aqueous bicarbonate and BiO_x/ionic liquid/gas-phase CO_2 catalyst/catholyte compositions. Catalysts were deposited on a carbon paper gas diffusion layer to afford high surface area and to enable rapid mass transport of gas-phase CO_2 under acidic conditions. We show that high current densities and stable operation can be achieved for the production of CO + H_2 mixtures in these BPM-based cells.

Figure 1 shows electron micrographs and cyclic voltammetric data for $NiFeO_x$ and Ag nanoparticle catalysts supported on

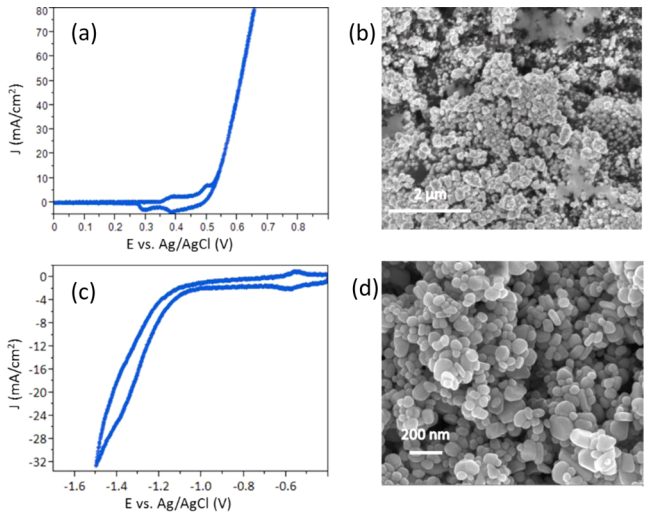

Figure 1. Cyclic voltammetric scans (20 mV/s) and SEM images of supported anode and cathode catalysts: (a) OER at the $NiFeO_x$ catalyst on carbon paper in 1 M NaOH; (b) SEM image of the electrodeposited $NiFeO_x$ on carbon paper; (c) CO_2RR at the Ag catalyst on carbon paper in 0.5 M $KHCO_3$; and (d) SEM image of the Ag nanoparticle catalyst on carbon paper.

porous carbon paper. Both electrocatalysts consist of aggregates of nanoparticles with diameters in the range of 10−100 nm. The OER and CO_2RR performance of the $NiFeO_x$ and Ag catalysts were characterized separately by cyclic voltammetry in three-electrode cells (see the Supporting Information). The $NiFeO_x$ catalyst showed anodic and cathodic waves characteristic of the Ni(II/III) couple at 0.4−0.5 V[32,33] and gave a current density of 80 mA/cm^2 at +0.65 V vs Ag/AgCl (η_{OER} = 400 mV) in 1.0 M NaOH. The Ag catalyst had a CO_2RR onset potential of −1.05 V vs Ag/AgCl in aqueous $KHCO_3$ and a current density of 30 mA/cm^2 at −1.5 V. The activity of both catalysts was thus comparable to those previously reported in the literature under similar conditions.[13,21]

CO_2 electrolysis using $NiFeO_x$ and Ag catalysts was first studied in a sandwich cell in which the catalytic electrodes, in contact with liquid electrolytes, were separated by a membrane. Aqueous 0.5 M $KHCO_3$ saturated with CO_2 and 0.1 M KOH were circulated through the serpentine cathode and anode flow fields, respectively, by means of peristaltic pumps. A BPM (Fumasep) was compared with a commercial Nafion cation exchange membrane and a Neosepta anion exchange membrane (AEM), and the results are shown in Figure 2. The onset

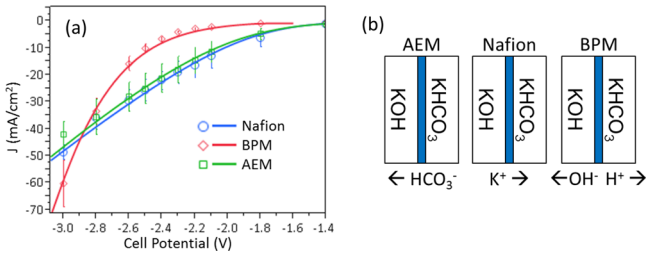

Figure 2. (a) j−V curves of the CO_2 electrolyzer with AEM, Nafion, and BPM membranes. KOH (0.1 M) was used as the anolyte and 0.5 M $KHCO_3$ bubbled with CO_2 gas was used as the catholyte. (b) Illustration of the predominant ion transport processes during electrolyzer operation with AEM, Nafion, and bipolar membranes.

potentials for CO_2 electrolysis with the AEM and Nafion membranes were −1.6 V, whereas for the BPM membrane the onset was at about −2.2 V. The difference in the onset potentials reflects the fact that, in the case of the AEM and Nafion membranes, an additional thermodynamic driving force is being applied to the cell by acid−base neutralization. For example, in the Nafion cell, the oxidation of water occurs at pH 13 and the reduction of CO_2 at pH ∼ 6 as K^+ ions are driven through the membrane. The overall reaction

$$8HCO_3^- + 4OH^- = 2CO + 6CO_3^{2-} + 6H_2O + O_2 \quad (1)$$

reflects the generation of four equivalents of acid at the anode, where OH^- is converted to H_2O and O_2 (reaction 2) and four of base at the cathode, where HCO_3^- is converted to CO and CO_3^{2-} (reaction 3). The potential of the Nafion-based cell is not stable because the anolyte and catholyte pH become progressively more acidic and basic, respectively, as current is passed. In contrast, in the BPM cell, the dissociation of water (reaction 5) drives H^+ and OH^- ions toward the cathode and anode, respectively; therefore, the overall cell reaction is reaction 6 and the pH of the anode and cathode remain constant.

Anode:

$$4OH^- = O_2 + 2H_2O + 4e^- \quad (2)$$

Cathode:

$$4HCO_3^- + 4e^- + 4H^+ = 2CO + 2CO_3^{2-} + 4H_2O \quad (3)$$

$$2CO_2 + 2CO_3^{2-} + 2H_2O = 4HCO_3^- \quad (4)$$

Bipolar membrane:

$$4H_2O = 4H^+ + 4OH^- \quad (5)$$

Overall:

$$2CO_2 = 2CO + O_2 \quad (6)$$

In addition, a loss of ∼300 mV occurs in the BPM cell because of the reaction of protons with HCO_3^- ions at the membrane/catholyte

DOI: 10.1021/acsenergylett.6b00475
ACS Energy Lett. 2016, 1, 1149−1153

interface, as shown schematically in Figure 2b (see also Figure S2). Fitting of the data in Figure 2 to Tafel kinetics with series resistance (see the Supporting Information) gave E^{o} values of 1.37, 1.57, and 1.99 V for the AEM, Nafion, and BPM cells, respectively. The series resistances, translated to area-specific resistances of the membranes, were 16 and 18 $\Omega \cdot cm^2$ for the AEM and Nafion, respectively, and 1.7 $\Omega \cdot cm^2$ for the BPM.

Figure 3a shows the Faradaic efficiencies (FE) for CO_2 reduction to CO and water reduction to H_2 at the Ag catalyst

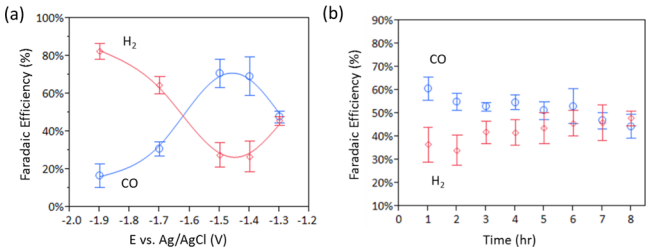

Figure 3. (a) FE of the Ag catalyst tested in 0.5 M $KHCO_3$ in a three-electrode configuration. (b) FE of the Ag catalyst in the BPM-based liquid cell electrolyzer measured at a constant current density of 50 mA/cm^2. The anode electrolyte was 0.1 M KOH, and the cathode electrolyte was 0.5 M $KHCO_3$.

in 0.5 M $KHCO_3$ electrolyte. The FE of CO reached a maximum at a cathode potential of −1.45 V vs Ag/AgCl and decreased at higher overpotentials. The sum of the CO and H_2 FE was close to 100% at all potentials. The voltage-dependent FE for the Ag catalyst is consistent with earlier reports.[21] Figure 3b shows the time dependence of the FE of the Ag catalyst in the full BPM liquid cell with a $NiFeO_x$ anode at 50 mA/cm^2 current density. Initially, the CO selectivity was above 60%. This corresponds to about 30 mA/cm^2 for CO_2 reduction to CO, which agrees well to the maximum current density expected from the solubility of CO_2 in the liquid electrolyte.[34,35] The FE for CO production declined slowly over 8 h and the hydrogen FE increased correspondingly. Several mechanisms for the drop in CO selectivity have been proposed previously.[36−38] The most likely cause is the deposition of impurity ions from the electrolyte onto the catalyst surface and their promotion of the competing hydrogen evolution reaction.

In order to address the mass transport limitations of the CO_2 reduction in the liquid cell, as well as to avoid the free-energy loss associated with acid−base neutralization at the BPM/catholyte interface, we studied CO_2 electrolysis with a gas diffusion cathode. As illustrated in Figure 4a, aqueous KOH was used as the anolyte and humidified CO_2 gas was delivered to the cathode. CO_2 reduction occurs at the boundary between the membrane and the gas-fed catalyst. An electrochemically deposited BiO_x catalyst on carbon paper was used, and the ionic liquid $BMIM^+OTf^-$ was drop-cast onto the BiO_x surface as a cocatalyst to stabilize the CO_2^- intermediate.[10] BiO_x has been shown to be a highly effective catalyst for CO_2 reduction to CO when combined with alkylimidazolium cations.[3,8] We designed this electrolyzer to combine the advantages of earth-abundant, low-cost catalysts; long-term stability afforded by the BPM; and high current density afforded by the gas-fed CO_2 delivery. Figure 4b compares $j-V$ curves of the gas-fed cells with AEM, Nafion, and BPM. As in the liquid-phase cell, the BPM had lower resistance than the AEM or Nafion. The AEM had strikingly low current density, presumably because of the poor conductivity of the triflate anion and the rapid polarization of the membrane as base is produced at the cathode. Figure 4c shows a constant current

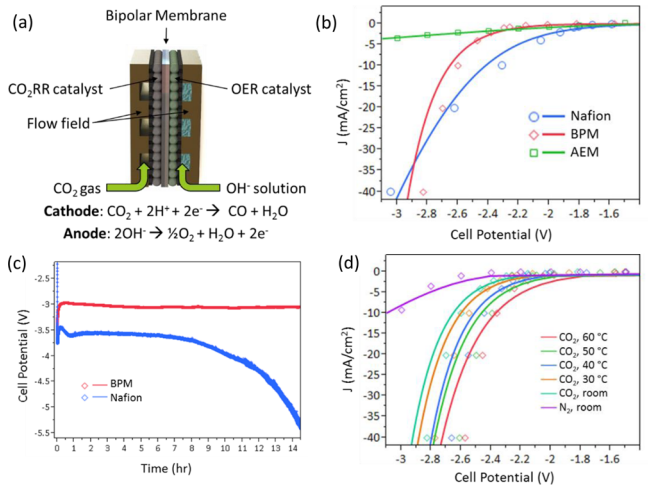

Figure 4. (a) Schematic drawing of a gas-fed CO_2 electrolyzer. Gaseous CO_2 was fed into the cathode through serpentine flow fields that contacted the porous carbon paper on which the BiO_x/$BMIM^+OTf^-$ catalyst was supported. (b) $j-V$ curves for the gas-fed cell comparing BPM, AEM, and Nafion membranes. Lines represent best fits to Tafel kinetics with series resistance. (c) Stability comparison between BPM and Nafion membrane at 80 mA/cm^2. (d) Gas-fed BPM-based electrolyzer operated at different temperatures. Lines represent Tafel equation fits. See the Supporting Information for details.

comparison at 80 mA/cm^2 between the BPM and the Nafion membrane. The voltage of the BPM cell was stable throughout the 14 h test, whereas the Nafion membrane polarized rapidly and started to fail after 7 h because of the depletion of OH^- at the anode. Similar results were obtained in the liquid-phase cell (see Figure S3). Figure 4d shows results with the gas-fed CO_2 BPM-based electrolyzer operated at different temperatures. Current densities increased as the temperature increased from room temperature to 60 °C. When nitrogen gas was fed into the electrolyzer instead of CO_2, a much lower but still measurable current density was obtained because of the HER.

The stability of the Faradaic efficiency is currently problematic with the gas-fed electrolyzer design. In a typical test such as that shown in Figure 4c, both CO and hydrogen are detected at the beginning of the reaction, but the CO FE deteriorates within 1 h. This is likely due to dewetting of the ionic liquid from the catalyst surface. The flow of humidified CO_2 may contribute to downstream convection of the ionic liquid in the cell. Drawing parallels to hydrogen−air fuel cell technologies, this situation might be improved by modifying the surface of the carbon support to promote wetting by the ionic liquid or by binding appropriate cations directly to the catalyst or support. Experiments at higher applied voltages showed that mass transport limitations in the BPM-based gas-phase cell became apparent as the current density approached 200 mA/cm^2 (see Figure S4). While there is intensive effort devoted to discovering and developing CO_2RR catalysts, very few studies have investigated system-level issues and designs for CO_2 electrolysis at such high current densities. The gas-fed BPM-based electrolyzer holds promise for carrying out the CO_2RR at practical current densities for long periods of time if the remaining engineering challenges can be met.

■ ASSOCIATED CONTENT

Supporting Information

The Supporting Information is available free of charge on the ACS Publications website at DOI: 10.1021/acsenergylett.6b00475.

DOI: 10.1021/acsenergylett.6b00475
ACS Energy Lett. 2016, 1, 1149−1153

Experimental details, catalyst characterization data, stability comparison of Nafion and bipolar membranes for liquid cell electrolysis, $j-V$ curve fitting parameters, and $j-V$ data for the gas-fed bipolar membrane cell at high bias (PDF)

AUTHOR INFORMATION

Corresponding Author

*E-mail: tem5@psu.edu.

ORCID

Yuguang C. Li: 0000-0002-9559-7051
Curtis P. Berlinguette: 0000-0001-6875-849X
Thomas E. Mallouk: 0000-0003-4599-4208

Notes

The authors declare no competing financial interest.

ACKNOWLEDGMENTS

This work was supported by the Office of Basic Energy Sciences, Division of Chemical Sciences, Geosciences, and Energy Biosciences, Department of Energy, under Contract DE-FG02-07ER15911, and by the Canadian Institute for Advanced Research. D.A.S. gratefully acknowledges support from the Killam Trusts.

REFERENCES

(1) Asadi, M.; Kim, K.; Liu, C.; Addepalli, A. V.; Abbasi, P.; Yasaei, P.; Phillips, P.; Behranginia, A.; Cerrato, J. M.; Haasch, R.; et al. Nanostructured Transition Metal Dichalcogenide Electrocatalysts for CO_2 Reduction in Ionic Liquid. *Science* **2016**, *353*, 467−470.

(2) Asadi, M.; Kumar, B.; Behranginia, A.; Rosen, B. A.; Baskin, A.; Repnin, N.; Pisasale, D.; Phillips, P.; Zhu, W.; Haasch, R.; et al. Robust Carbon Dioxide Reduction on Molybdenum Disulphide Edges. *Nat. Commun.* **2014**, *5*, 4470.

(3) DiMeglio, J. L.; Rosenthal, J. Selective Conversion of CO_2 to CO with High Efficiency Using an Inexpensive Bismuth-Based Electrocatalyst. *J. Am. Chem. Soc.* **2013**, *135*, 8798−8801.

(4) Kuhl, K. P.; Cave, E. R.; Abram, D. N.; Jaramillo, T. F. New Insights into the Electrochemical Reduction of Carbon Dioxide on Metallic Copper Surfaces. *Energy Environ. Sci.* **2012**, *5*, 7050−7059.

(5) Kumar, B.; Asadi, M.; Pisasale, D.; Sinha-Ray, S.; Rosen, B. A.; Haasch, R.; Abiade, J.; Yarin, A. L.; Salehi-Khojin, A. Renewable and Metal-free Carbon Nanofibre Catalysts for Carbon Dioxide Reduction. *Nat. Commun.* **2013**, *4*, 2819.

(6) Li, C. W.; Kanan, M. W. CO_2 Reduction at Low Overpotential on Cu Electrodes Resulting from the Reduction of Thick Cu_2O Films. *J. Am. Chem. Soc.* **2012**, *134*, 7231−7234.

(7) Liu, M.; Pang, Y.; Zhang, B.; De Luna, P.; Voznyy, O.; Xu, J.; Zheng, X.; Dinh, C. T.; Fan, F.; Cao, C.; et al. Enhanced Eelectrocatalytic CO_2 Reduction via Field-induced Reagent Concentration. *Nature* **2016**, *537*, 382−386.

(8) Medina-Ramos, J.; DiMeglio, J. L.; Rosenthal, J. Efficient Reduction of CO_2 to CO with High Current Density Using in Situ or ex Situ Prepared Bi-Based Materials. *J. Am. Chem. Soc.* **2014**, *136*, 8361−8367.

(9) Rakowski Dubois, M.; Dubois, D. L. Development of Molecular Electrocatalysts for CO_2 Reduction and H_2 Production/Oxidation. *Acc. Chem. Res.* **2009**, *42*, 1974−1982.

(10) Rosen, B. A.; Salehi-Khojin, A.; Thorson, M. R.; Zhu, W.; Whipple, D. T.; Kenis, P. J. A.; Masel, R. I. Ionic Liquid Mediated Selective Conversion of CO_2 to CO at Low Overpotentials. *Science* **2011**, *334*, 643−644.

(11) Zhu, W.; Michalsky, R.; Metin, Ö.; Lv, H.; Guo, S.; Wright, C. J.; Sun, X.; Peterson, A. A.; Sun, S. Monodisperse Au Nanoparticles for Selective Electrocatalytic Reduction of CO_2 to CO. *J. Am. Chem. Soc.* **2013**, *135*, 16833−16836.

(12) McCrory, C. C. L.; Jung, S.; Ferrer, I. M.; Chatman, S. M.; Peters, J. C.; Jaramillo, T. F. Benchmarking Hydrogen Evolving Reaction and Oxygen Evolving Reaction Electrocatalysts for Solar Water Splitting Devices. *J. Am. Chem. Soc.* **2015**, *137*, 4347−4357.

(13) McCrory, C. C. L.; Jung, S.; Peters, J. C.; Jaramillo, T. F. Benchmarking Heterogeneous Electrocatalysts for the Oxygen Evolution Reaction. *J. Am. Chem. Soc.* **2013**, *135*, 16977−16987.

(14) Lau, G. P. S.; Schreier, M.; Vasilyev, D.; Scopelliti, R.; Grätzel, M.; Dyson, P. J. New Insights Into the Role of Imidazolium-Based Promoters for the Electroreduction of CO_2 on a Silver Electrode. *J. Am. Chem. Soc.* **2016**, *138*, 7820−7823.

(15) Rosen, B. A.; Haan, J. L.; Mukherjee, P.; Braunschweig, B.; Zhu, W.; Salehi-Khojin, A.; Dlott, D. D.; Masel, R. I. In Situ Spectroscopic Examination of a Low Overpotential Pathway for Carbon Dioxide Conversion to Carbon Monoxide. *J. Phys. Chem. C* **2012**, *116*, 15307−15312.

(16) Sun, L.; Ramesha, G. K.; Kamat, P. V.; Brennecke, J. F. Switching the Reaction Course of Electrochemical CO_2 Reduction with Ionic Liquids. *Langmuir* **2014**, *30*, 6302−6308.

(17) Alvarez-Guerra, M.; Albo, J.; Alvarez-Guerra, E.; Irabien, A. Ionic Liquids in the Electrochemical Valorisation of CO_2. *Energy Environ. Sci.* **2015**, *8*, 2574−2599.

(18) Delacourt, C.; Ridgway, P. L.; Kerr, J. B.; Newman, J. Design of an Electrochemical Cell Making Syngas (CO+ H_2) from CO_2 and H_2O Reduction at Room Temperature. *J. Electrochem. Soc.* **2008**, *155*, B42−B49.

(19) Dufek, E. J.; Lister, T. E.; McIlwain, M. E. Influence of Electrolytes and Membranes on Cell Operation for Syn-Gas Production. *Electrochem. Solid-State Lett.* **2012**, *15*, B48−B50.

(20) Shi, J.; Shi, F.; Song, N.; Liu, J.-X.; Yang, X.-K.; Jia, Y.-J.; Xiao, Z.-W.; Du, P. A Novel Electrolysis Cell for CO_2 Reduction to CO in Ionic Liquid/Organic Solvent Electrolyte. *J. Power Sources* **2014**, *259*, 50−53.

(21) Hatsukade, T.; Kuhl, K. P.; Cave, E. R.; Abram, D. N.; Jaramillo, T. F. Insights into the Electrocatalytic Reduction of CO_2 on Metallic Silver Surfaces. *Phys. Chem. Chem. Phys.* **2014**, *16*, 13814−13819.

(22) Salehi-Khojin, A.; Jhong, H.-R. M.; Rosen, B. A.; Zhu, W.; Ma, S.; Kenis, P. J. A.; Masel, R. I. Nanoparticle Silver Catalysts That Show Enhanced Activity for Carbon Dioxide Electrolysis. *J. Phys. Chem. C* **2013**, *117*, 1627−1632.

(23) Hernández-Pagán, E. A.; Vargas-Barbosa, N. M.; Wang, T.; Zhao, Y.; Smotkin, E. S.; Mallouk, T. E. Resistance and Polarization Losses in Aqueous Buffer-membrane Electrolytes for Water-splitting Photoelectrochemical Cells. *Energy Environ. Sci.* **2012**, *5*, 7582−7589.

(24) Luo, J.; Vermaas, D. A.; Bi, D.; Hagfeldt, A.; Smith, W. A.; Grätzel, M. Bipolar Membrane-Assisted Solar Water Splitting in Optimal pH. *Adv. Energy Mater.* **2016**, *6*, 1600100.

(25) McDonald, M. B.; Ardo, S.; Lewis, N. S.; Freund, M. S. Use of Bipolar Membranes for Maintaining Steady-State pH Gradients in Membrane-Supported, Solar-Driven Water Splitting. *ChemSusChem* **2014**, *7*, 3021−3027.

(26) McDonald, M. B.; Bruce, J. P.; McEleney, K.; Freund, M. S. Reduced Graphene Oxide Bipolar Membranes for Integrated Solar Water Splitting in Optimal pH. *ChemSusChem* **2015**, *8*, 2645−2654.

(27) Reiter, R. S.; White, W.; Ardo, S. Electrochemical Characterization of Commercial Bipolar Membranes under Electrolyte Conditions Relevant to Solar Fuels Technologies. *J. Electrochem. Soc.* **2016**, *163*, H3132−H3134.

(28) Sun, K.; Liu, R.; Chen, Y.; Verlage, E.; Lewis, N. S.; Xiang, C. A Stabilized, Intrinsically Safe, 10% Efficient, Solar-Driven Water-Splitting Cell Incorporating Earth-Abundant Electrocatalysts with Steady-State pH Gradients and Product Separation Enabled by a Bipolar Membrane. *Adv. Energy Mater.* **2016**, *6*, 1600379.

(29) Vargas-Barbosa, N. M.; Geise, G. M.; Hickner, M. A.; Mallouk, T. E. Assessing the Utility of Bipolar Membranes for use in Photoelectrochemical Water-Splitting Cells. *ChemSusChem* **2014**, *7*, 3017−3020.

(30) Vermaas, D. A.; Sassenburg, M.; Smith, W. A. Photo-assisted Water Splitting with Bipolar Membrane Induced pH Gradients for Practical Solar Fuel Devices. *J. Mater. Chem. A* **2015**, *3*, 19556−19562.

DOI: 10.1021/acsenergylett.6b00475
ACS Energy Lett. 2016, 1, 1149−1153

(31) Zhou, X.; Liu, R.; Sun, K.; Chen, Y.; Verlage, E.; Francis, S. A.; Lewis, N. S.; Xiang, C. Solar-Driven Reduction of 1 atm of CO_2 to Formate at 10% Energy-Conversion Efficiency by Use of a TiO_2-Protected III−V Tandem Photoanode in Conjunction with a Bipolar Membrane and a Pd/C Cathode. *ACS Energy Lett.* **2016**, *1*, 764−770.
(32) Dionigi, F.; Strasser, P. NiFe-Based (Oxy) hydroxide Catalysts for Oxygen Evolution Reaction in Non-Acidic Electrolytes. *Adv. Energy Mater.* **2016**, 1600621.
(33) Louie, M. W.; Bell, A. T. An Investigation of Thin-Film Ni−Fe Oxide Catalysts for the Electrochemical Evolution of Oxygen. *J. Am. Chem. Soc.* **2013**, *135*, 12329−12337.
(34) Hori, Y. In *Modern Aspects of Electrochemistry*; Vayenas, C. G., White, R. E., Gamboa-Aldeco, M. E., Eds.; Springer: New York, 2008; pp 89−189.
(35) Lu, Q.; Jiao, F.Electrochemical CO_2 Reduction: Electrocatalyst, Reaction Mechanism, and Process Engineering. *Nano Energy* **2016**, http://dx.doi.org/10.1016/j.nanoen.2016.04.009.
(36) Hori, Y.; Konishi, H.; Futamura, T.; Murata, A.; Koga, O.; Sakurai, H.; Oguma, K. Deactivation of Copper Electrode" in Electrochemical Reduction of CO_2. *Electrochim. Acta* **2005**, *50*, 5354−5369.
(37) Wu, J.; Sun, S.-G.; Zhou, X.-D. Origin of the Performance Degradation and Implementation of Stable Tin Electrodes for the Conversion of CO_2 to Fuels. *Nano Energy* **2016**, *27*, 225−229.
(38) Xie, J.-F.; Huang, Y.-X.; Li, W.-W.; Song, X.-N.; Xiong, L.; Yu, H.-Q. Efficient Electrochemical CO_2 Reduction on a Unique Chrysanthemum-like Cu Nanoflower Electrode and Direct Observation of Carbon Deposite. *Electrochim. Acta* **2014**, *139*, 137−144.

DOI: 10.1021/acsenergylett.6b00475
ACS Energy Lett. 2016, 1, 1149−1153